Design of thermal cloaks with isotropic materials based on machine learning

Qingxiang Ji[a], Yunchao Qi[a], Chenwei Liu[a], Songhe Meng[a], Jun Liang[b,*], Muamer Kadic [c], Guodong Fang[a,*]

[a] *National Key Laboratory of Science and Technology on Advanced Composites in Special Environments, Harbin Institute of Technology, Harbin, 150001, China*

[b] *Institute of Advanced Structure Technology, Beijing Institute of Technology, Beijing 100081, China*

[c] *Institute FEMTO-ST, CNRS, University Bourgogne Franche-Comté, 25000, Besançon, France*

Abstract

Thermal manipulation has been widely researched due to its potentials in novel functions, such as cloaking, illusion and sensing. However, thermal manipulation is often realized by metamaterials which entails extreme material properties. Here, we propose a machine learning based thermal cloak consisting of a finite number of layers with isotropic materials. An artificial neural network is established to intelligently learn the relation between each layer's constitutive properties and the cloaking performances. Optimal material properties are retrieved so that heat flows can be directed to detour the cloaked object without any invasion, as if the object is not there. The designed cloak demonstrates both easiness to implement in applications and excellent performances in thermal invisibility, which are verified by simulations and experiments. The proposed method can be flexibly extended to other physical fields, like acoustics and electromagnetics, providing inspiration for metamaterials design in a wide range of communities.

Keywords: Transformation thermotics; Thermal cloak; Artificial neural network

1. Introduction

Thermal manipulation has recently attracted wide attention and researches following the pioneering works of transformed theory [1, 2, 3, 4, 5, 6]. Many novel thermal meta-devices are created, like invisible cloaks, sensors and illusion devices [7, 8, 9, 10, 11, 12, 13, 14, 15, 16, 17]. Thermal meta-devices face the challenge of extreme constitutive properties. Most reported devices are realized by metamaterials with unconventional thermal conductivity, i.e., anisotropic and graded. Yet practical applications desire materials with realistic physical properties. Researchers have proposed many fruitful strategies to design thermal meta-devices with bulky material compositions, such as composite structures design [8, 18, 19, 20], scattering-cancellation approach [21, 22, 23, 24] and neutral inclusion method [25, 26, 27, 28]. However, these design schemes are still not easy to implement, as they need complex alternating layer shapes or they have low topological property and finite functionalities. Considering that these direct strategies possess drawbacks in technical realization, researchers have developed inverse design methodology. Inverse design approach features its advantage over other methods in that it allows to take into account various kinds of constraints on solutions including those related to technical realization [29, 30]. Topology optimization is introduced into the inverse design of thermal meta-devices, demonstrating simplified material properties and excellent performances [31, 32, 33, 34], whereas, topology optimization method usually results in complex structural configuration that imposes difficulties to fabrications. In addition, conventional optimization usually encounters the local minima problem and needs a well-defined objective function for accurate design

[1] liangjun@bit.edu.cn, fanggd@hit.edu.cn

[35]. New design schemes are required with the purpose to simplify engineering preparations and reduce the computational workloads.

In this work, we propose a data driven approach to design thermal cloaks with bulk isotropic materials. A multilayered concentric cloak is designed where each layer is composed of different isotropic materials. An artificial neural network is proposed and trained to intelligently learn the intrinsic relation between input material parameters and their influences on cloaking performances [35, 36]. The network proves effective by accurately learning intrinsic relations from a small number of samples, and is efficient in significantly reducing computation time by predicting solutions immediately after the training phase [35]. By using deep learning we have exploited the intricate relationship between each layer's material properties and general cloaking performances. Optimal material properties of each layer are retrieved, and the optimized thermal cloak not only simplifies practical fabrication, but demonstrates excellent heat cloaking effects in both simulations and experiments.

2. Methods and results

2.1. Design scheme

We consider a cylindrical thermal cloak with a concentric shell configuration. The goal is to render the object (indicated in white in Fig. 1a) thermally invisible, without disturbing original thermal profiles. Basically, one can achieve this goal in one of following ways: preset layer thickness and find the optimal material properties, or choose shell materials and determine the optimal layer thickness, or use both layer thickness and material properties as design variables. Here we choose the first approach and build a thermal cloak with four layers where each layer is made of different materials but with equal thickness, as illustrated in Fig. 1a. The design space is characterized by each layer's thermal conductivity k_m, where m is the layer index. Note that the deep learning model (as shown later) is readily applicable to thermal cloaks with different number of layers.

The heat conduction equation in cylindrical system is expressed as

$$\frac{\partial^2 T_0}{\partial r^2} + \frac{1}{r}\frac{\partial T_0}{\partial r} + \frac{1}{r^2}\frac{\partial^2 T_0}{\partial \theta^2} = 0 \tag{1}$$

$$\frac{\partial^2 T_m}{\partial r^2} + \frac{1}{r}\frac{\partial T_m}{\partial r} + \frac{1}{r^2}\frac{\partial^2 T_m}{\partial \theta^2} = 0 \tag{2}$$

where the subscript 0 denote the central region and $m = 1, 2, 3, 4, 5$ denote regions from the center to outermost.

Considering the symmetry of boundary conditions, the temperature distributions in different regions can be expressed as

$$T_0 = A_0 + B_0 r\cos\theta + C_0 r^{-1}\cos\theta, \tag{3}$$

$$T_m = A_0 + B_m r\cos\theta + C_m r^{-1}\cos\theta, \tag{4}$$

where A_0 is the known temperature of the central point, B_0, B_m and C_m are unknown coefficients to be determined.

Boundary continuity conditions of temperature and normal heat flux require

$$\begin{cases} T_{m-1}\big|_{r=r_m} = T_m\big|_{r=r_m} \\ -k_{m-1}\nabla T_{m-1}\big|_{r=r_m} = -k_m \nabla T_m\big|_{r=r_m} \end{cases}. \tag{5}$$

Combining Eq. (4) and Eq. (5), we obtain the simplified form

$$\begin{cases} B_{m-1} r_m + C_{m-1} r_m^{-1} = B_m r_m + C_m r_m^{-1} \\ -k_{m-1}\left(B_{m-1} - C_{m-1} r_m^{-2}\right) = -k_m\left(B_m - C_m r_m^{-2}\right) \end{cases} \tag{6}$$

Generally, a thermal cloak should accomplish following goals: (a) guiding heat flows to detour without invading the object; (b) directing heat flows to return to their original paths without disturbing external thermal profiles. Considering perfect thermal neutrality effects (no perturbations to external thermal field), we have $C_0 = C_5 = 0$, and B_5 can be easily obtained by the applied uniform thermal gradient. We now have nine unknown coefficients to be determined but have ten equations, which will result in a matching condition between material properties k_0, k_m and geometry parameters r_i (see the supporting information). Thermal cloaking effects are achieved if all the material properties and structural parameters completely match this criterion. In theory, we

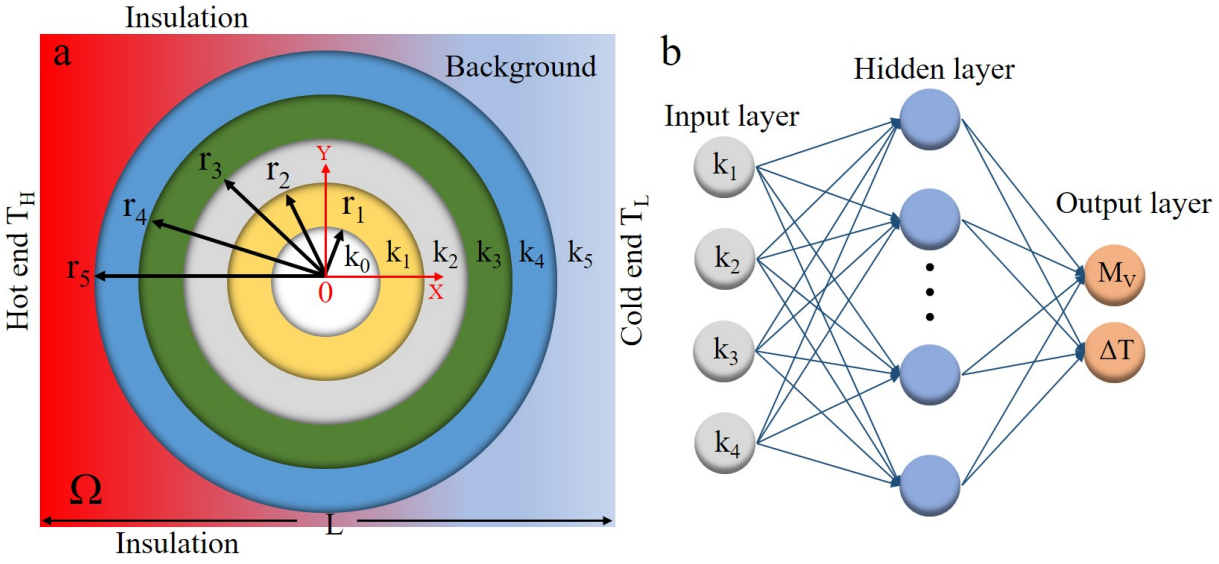

Fig. 1. Framework of the deep learning model for the design of thermal cloaks. (a) The design scheme. (b) The artificial neural network.

can find the analytical expression of Eq. (6). However, it may be tough to determine the material properties that simultaneously achieve undisturbed external fields and zero temperature variations in the central region, especially in the case of large number of layers, more complicated shapes or under material property constraints. Besides, the material properties are associated with each other and there may exist multiple potential solutions. The influences of material properties k_m on thermal cloaking performances can be revealed intuitively by Eq. (6). A practical implementation may demand flexibility in the design due to external perturbation, i.e., unavailability of material properties. For a given object and predefined geometry, the analytical solution may be not well-satisfied due to such external perturbations, hence a local optimal solution is indeed needed. We notice that there exists a mapping relation between each layer's materials properties and the cloaking performances. Hence we turn the inverse problem into an optimization problem and reversely design the material properties that results in thermal cloaking effects.

To quantitatively demonstrate the thermal cloaking effects, two objective functions are defined, one to characterize the thermal difference within the object domain:

$$\Delta T = \left| T_{x=r_1} - T_{x=-r_1} \right|, \tag{7}$$

and the other to characterize thermal neutrality of the cloak:

$$M_V = \frac{\int_\Omega |T(x,y,z) - T_r(x,y,z)|\, d\Omega}{\int_\Omega d\Omega}, \tag{8}$$

where Ω represents the probe domain of external fields $r > r_5$, and T_r denotes the reference thermal field of a homogeneous plate as $T_r = T_H - \frac{T_H - T_L}{L}(x + \frac{L}{2})$.

In our design, thermal properties of the central region and background region are respectively $k_0 = 394\ \mathrm{Wm^{-1}K^{-1}}$ and $k_5 = 77.6\ \mathrm{Wm^{-1}K^{-1}}$, the side-length is $L = 0.125$ m, the inner radius is $r_1 = 0.025$ m and the outer radius $r_5 = 0.05$ m. Considering fabrication easiness and availability, we have defined ranges of the design parameters as $0.15 < k_1 < 27$, $360 < k_2 < 394$, $0.15 < k_3 < 27$, $360 < k_4 < 394$ in units of $\mathrm{Wm^{-1}K^{-1}}$ [8]. We mention by passing that broader ranges may decrease the prediction efficiency, but this can be compensated by building more data samples. We denote the original design space by the symbol $D^0 = \{k_1, k_2, k_3, k_4\}$. The goal is to find an optimal set of parameters k_m within the

constraint design space $D^0 = \{k_1, k_2, k_3, k_4\}$. Generally, the optimization objective should be illustrated as:

$$\begin{aligned} &\min M_V \\ &\min \Delta T \\ &\text{S.t. } k_m \in D^0. \end{aligned} \tag{9}$$

Perfect cloaking performances are achieved when optimized design parameters yield zero M_V and ΔT. However, we notice that M_V and ΔT may achieve minimal values at different points, rendering no solutions to Eq. (9). Therefore, the objective is accomplished in following two steps.

First, we obtain a design space D^* within which the samples have values of M_V infinitely approach the minimal value, which can be illustrated as:

$$\begin{aligned} &M_V \rightarrow M_V^{min} \\ &\text{S.t. } k_m \in D^0. \end{aligned} \tag{10}$$

where M_V^{min} denotes the minimum value within the samples space D^0.

Then we search for the optimal design parameters that yields minimum ΔT within the design space D^*, which can be illustrated as:

$$\begin{aligned} &\min \Delta T \\ &\text{S.t. } k_m \in D^*. \end{aligned} \tag{11}$$

2.2. Artificial neural network

We propose an artificial neural network to learn the intrinsic relations between the design parameters and the thermal cloaking performances (see Fig. 1b). The forward neural network maps the design space $[k_1, k_2, k_3, k_4]$ (the input layer) to the results space $[M_V,\ \Delta T]$ (the output layer). For the hidden layer, the number of layer nodes is determined by an empirical formula:

$$N = \sqrt{n_1 + n_2} + \delta, \tag{12}$$

where n_1 and n_2 are the number of layer nodes for the input layer and output layer, respectively, δ is an empirical constant. We obtain the number of layer nodes $N = 6$ following Eq. 12. Details about the structure of the artificial neural network can be found in the supporting information.

Optimal Latin hypercube sampling technique is used to obtain 1000 sample control points. The created sample points spread evenly in the design space, which adds more prediction accuracy to the deep learning model. We solved the direct problem $[k_1, k_2, k_3, k_4]$ numerically by the commercial software COMSOL Multiphysics and got corresponding values of M_V and ΔT for the control points. We train the artificial neural network with the relation from each layer's material properties to the cloaking performances using the obtained samples, which are split into three sets: for training (70%), for validation (15%) and for final testing (15%), respectively. The input data are normalized and then fed into the network to expedite the convergence of the algorithm. Mean square error (MSE) is used as the loss function between the predicted and desired output. However, we notice that it is impossible to build an effective prediction model between the input parameters and the two output index (see the supporting information). This is physically explained by the fact that there does not exist a well-predicted intrinsic relation between each layer's material properties k_m and thermal difference ΔT. Therefore, we instead establish the artificial neutral network only predicting the dependence of thermal neutrality of M_V on material properties k_m. Levenberg-Marquardt algorithm is selected as the training algorithm. The loss functions of training , validation and testing set vary with the number of iterations as shown in Fig. 2a. The loss function converges gradually after 400 epochs, implying completion of the training phase. The three loss function match well with each other, indicating that the artificial neural network is smooth without overfitting. Mean relative errors (MRE) on the samples are shown in Fig. 2(b-d) and listed in the inset table, where we observe that all the three sets of MREs are less than 2.3%. These results demonstrate high prediction accuracy and reliability of the artificial neural network on single output layer M_V.

We then turn to consider the output parameter ΔT. In practice, feasible material parameters are often desired with least temperature differences ΔT. Yet it is ineffective here to directly train the proposed artificial neural network in an inverse direction, either to derive a set of optimal design parameters $D = [k_1, k_2, k_3, k_4]$ from the target functions $R = [\Delta T, M_V]$

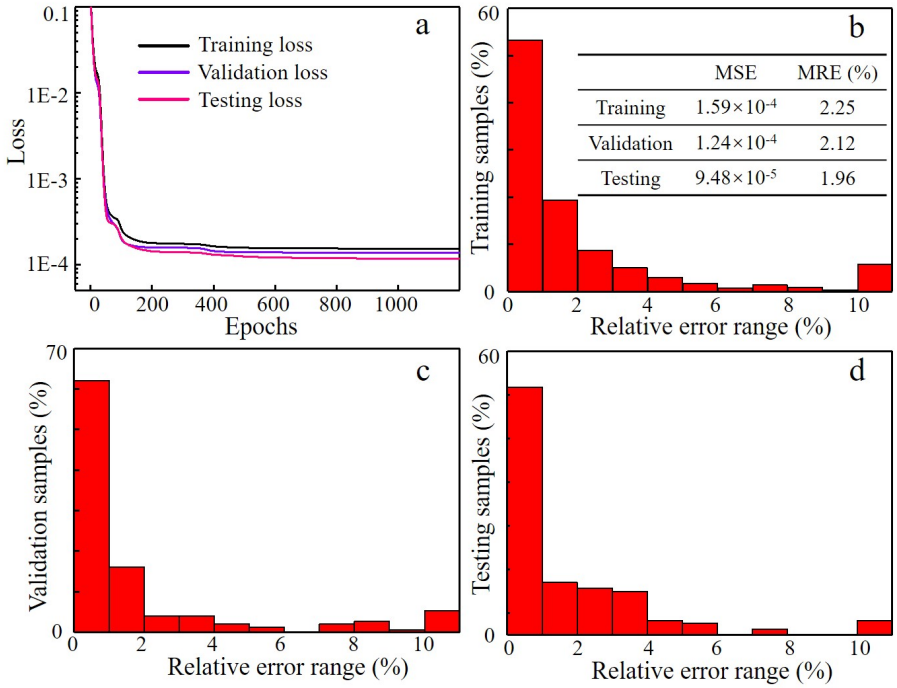

Fig. 2. Artificial neural network learning process. (a) The learning curves as a function of training epochs. (b) Histogram of relative errors for the testing samples.

by an inverse-mapping. To avoid such a pitfall, we generate a new set of 10000 design samples as the input of the network, using the relation we have established between M_V and k_m. Note that M_V of the 1000 original samples are got by finite element method, while for the 10000 new samples, the objective function M_V are obtained by the network directly. The process of searching for the optimal values is completed in the 10000 new samples. Considering that ΔT is not well-predictable by the artificial network, we first filter out the 1% samples that result in least M_V values and finally obtain the particular set of parameter that yields minimal ΔT from the selected 1% samples. We note by passing that it takes 76 seconds to generate the 10000 new samples by the network, whereas finite element analysis requires around 13 minutes.

We obtain one set of optimal design parameters as $k_1 = 23.11$, $k_2 = 386.58$, $k_3 = 5.91$ and $k_4 = 394$ in units of $\mathrm{Wm^{-1}K^{-1}}$. To verify the design method effective, we establish a thermal cloak of which each layer is constituted by the optimal material properties. We conduct numerical simulations and compare the results with the ideal cloak, the bare obstacle case and the homogeneous plate (see Fig. 3). Note that the ideal cloak here refers to a thermal cloak designed by transformation thermotics theory [1, 4]. It is observed that the optimized thermal cloak successfully guides heat flows to pass around the object and return to their original paths. For the optimized cloak, the temperature field in probe domain Ω shows few perturbations and are analogous to the field generated by the homogeneous plate. By contrast, the thermal field are drastically distorted in the case of a bare object. In addition, the optimized thermal cloak closely mimics the ideal cloak and significantly reduces the temperature differences in the inner domain, validating effectiveness of the design. We conduct quantitative analysis and show the calculated objective functions for different cases, as shown in Tab. 1. The results clearly show that the designed cloak significantly reduces the heat flux that invades the object and demonstrates excellent neutrality performances.

3. Experimental validation

The material properties of each layer and the background medium are not readily available by naturally existing materials. To obtain desired thermal con-

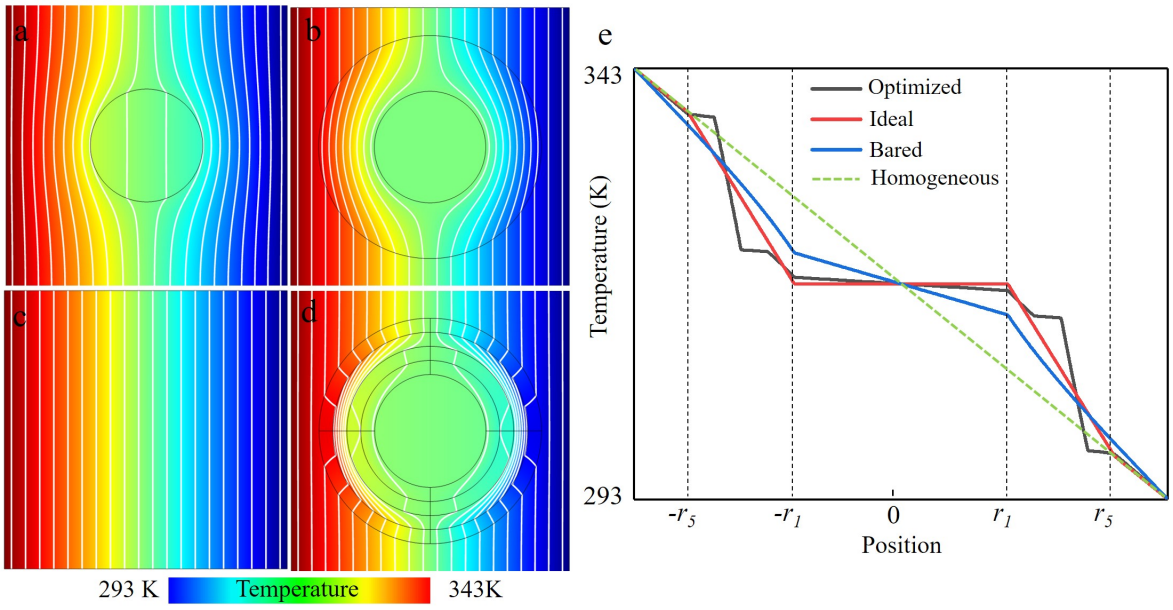

Fig. 3. Thermal profile for (a) the bare obstacle, (b) ideal thermal cloak, (c) the homogeneous plate and (d) the optimized cloak; (e) corresponding temperature profile along the observed line $y = 0$.

Table 1
Comparison of cloaking performances for different cloaks.

	Ideal cloak	Homogeneous plate	Bare obstacle	Optimized cloak
M_V (K)	4.9×10^{-7}	7.6×10^{-10}	1.3	0.1
ΔT (K)	0	20	7.2	1.5

ductivity, we design composite structures by drilling holes into the copper plate (thermal conductivity k_c = 394 $\mathrm{Wm^{-1}K^{-1}}$, thickness 2 mm) and filling them with polydimethylsiloxane (PDMS, thermal conductivity k_p = 0.15 $\mathrm{Wm^{-1}K^{-1}}$) [8]. For example, background heat conductivity k_5 is achieved by building holes array (holes diameter 1.8 mm) with equal space (2 mm). The holes array parameters are obtained following Maxwell-Garnett theory which is expressed $k_5 = k_c\left[1 + \frac{2(k_p-k_c)f}{k_p+k_c-(k_p-k_c)f}\right]$, where f denotes holes area fraction. The sample is manufactured by CNC machining technique, as shown in Fig. 4. Note that refined circular discretization of each layer can better approximate the required thermal properties, but at the same time results in more fabrication complexity. We have fabricated a thermal cloak with finite holes or arc grooves shown in Fig. 4c as a good trade-off.

In Fig. 4, we show the experimental system used to verify the performances of the designed thermal cloak. An infrared thermal camera (FLIR A6702sc) is used to capture thermal images via Planck thermal emission. The hot and cold ends are realized by thermostat water bath, remaining sides are left open and covered with PDMS layer of thickness around 1 mm. Heat convection between the samples and the surroundings are significantly reduced by this PDMS layer.

In Fig. 5, we show the numerical and experimental results for the proposed thermal cloak. It is observed that the thermal cloak successfully fulfills its task in that heat flux are guided to pass around the central region without invasion. The heat density are reduced in the central region than its surroundings. Furthermore, the temperature field outside of the device are almost not affected, as if nothing was there. Quantitative results plotted in Tab. 2 further verified the effectiveness of our designed cloak, where both temperatures difference in the central region and external temperature perturbations are minimized. The experimental results agree well with simulation re-

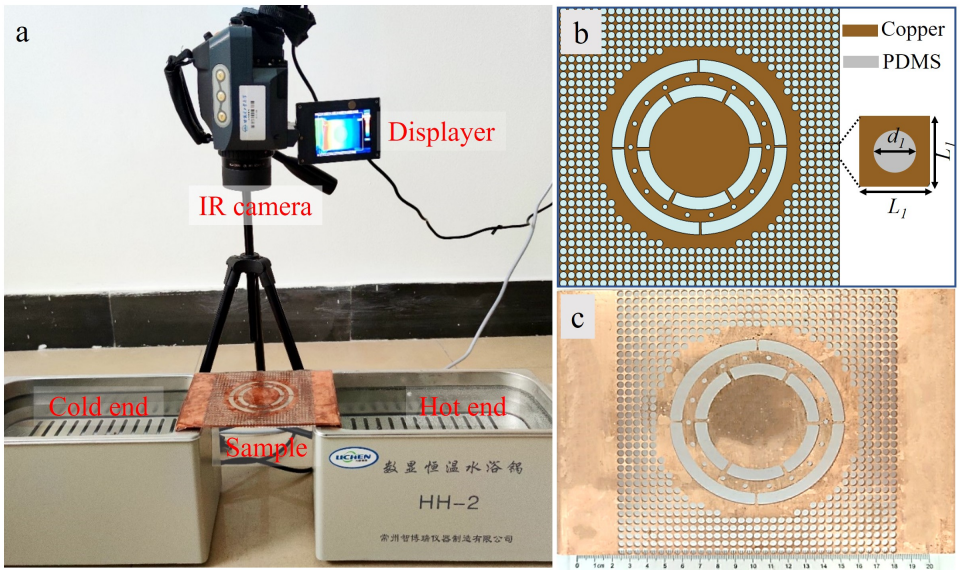

Fig. 4. The experimental system. (a) An infrared thermal camera is used to capture thermal images. The designed thermal cloak: (a) the numerical model and (b) the photograph.

sults, indicating the accuracy of the artificial neural network enabled design approach. We note slight discrepancies between simulations (see Tab. 1) and experimental results (see Tab. 2). The difference is mainly caused by fabrication errors and inaccuracy in temperature controlling systems.

Table 2
Experimental results of the cloaking performances, with the bare obstacle case as reference.

	Bare obstacle	Ideal cloak
M_V (K)	1.38	0.11
ΔT (K)	5.4	2.2

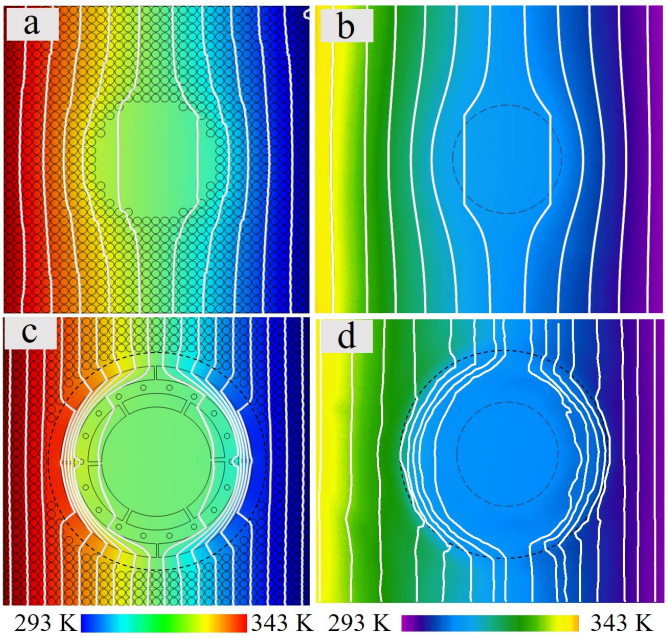

Fig. 5. Simulated and measured temperature distributions: (a) simulated results for a bare obstacle; (b) Experimental results for a bare obstacle; (c) simulated results for the designed cloak; (d) Experimental results for a bare obstacle. The white lines denote iso-temperature lines. The object and cloak are outlined by black dash lines.

4. Conclusion

We have proposed the design method of a multi-layered thermal cloak with core-shell configuration driven by deep learning. In particular, we establish an artificial neural network to predict the cloaking responses for given material properties. Optimal material properties are retrieved for target cloaking effects. We implement an optimized thermal cloak with bulk isotropic materials and verify excellent heat cloaking performances by both simulations and experiments, validating the effectiveness of our design method. The proposed method can be extended to other static physical fields, such as acoustic waves and electromagnetic field, suggesting an efficient route to design cloaks and related meta-devices.

CRediT authorship contribution statement

Qingxiang Ji: Conceptualization, Formal analysis, Writing original draft. **Yunchao Qi:** Methodology, Software. **Chenwei Liu:** Formal analysis, Writing original draft. **Songhe Meng:** Investigation, Visualization, Validation, Data curation. **Jun Liang:** Investigation, Visualization, Project administration. Muamer Kadic: Simulations and revision. **Guodong Fang:** Supervision, Project administration, Review and editing.

Declaration of Competing Interest

The authors declare that they have no known competing financial interests or personal relationships that could have appeared to influence the work reported in this paper.

Acknowledgments

This work was supported by the National Natural Science Foundation of China (Grant Nos. 11732002 and 12090034). We are also grateful to Natural Science Foundation of Heilongjiang Province of China (Grant Nos. YQ2021A004).

References

[1] J. B. Pendry, D. Schurig, D. R. Smith, Controlling electromagnetic fields, Science 312 (5781) (2006) 1780–1782.

[2] C. Fan, Y. Gao, J. Huang, Shaped graded materials with an apparent negative thermal conductivity, Applied Physics Letters 92 (25) (2008) 251907.

[3] T. Chen, C.-N. Weng, J.-S. Chen, Cloak for curvilinearly anisotropic media in conduction, Applied Physics Letters 93 (11) (2008) 114103.

[4] S. Guenneau, C. Amra, D. Veynante, Transformation thermodynamics: cloaking and concentrating heat flux, Optics Express 20 (7) (2012) 8207–8218.

[5] M. Farhat, S. Guenneau, S. Enoch, Ultrabroadband elastic cloaking in thin plates, Physical Review Letters 103 (2) (2009) 024301.

[6] M. Kadic, T. Bückmann, R. Schittny, M. Wegener, Metamaterials beyond electromagnetism, Reports on Progress in physics 76 (12) (2013) 126501.

[7] M. Kadic, S. Guenneau, S. Enoch, S. A. Ramakrishna, Plasmonic space folding: Focusing surface plasmons via negative refraction in complementary media, ACS nano 5 (9) (2011) 6819–6825.

[8] R. Schittny, M. Kadic, S. Guenneau, M. Wegener, Experiments on transformation thermodynamics: molding the flow of heat, Physical Review Letters 110 (19) (2013) 195901.

[9] R. Schittny, M. Kadic, T. Bückmann, M. Wegener, Invisibility cloaking in a diffusive light scattering medium, Science 345 (6195) (2014) 427–429.

[10] X. Shen, J. Huang, Thermally hiding an object inside a cloak with feeling, International Journal of Heat and Mass Transfer 78 (2014) 1–6.

[11] T. Yang, X. Bai, D. Gao, L. Wu, B. Li, J. T. Thong, C.-W. Qiu, Invisible sensors: Simultaneous sensing and camouflaging in multiphysical fields, Advanced Materials 27 (47) (2015) 7752–7758.

[12] G. Xu, H. Zhang, Y. Jin, Achieving arbitrarily polygonal thermal harvesting devices with homogeneous parameters through linear mapping function, Energy Conversion and Management 165 (2018) 253–262.

[13] J. Qin, W. Luo, P. Yang, B. Wang, T. Deng, T. Han, Experimental demonstration of irregular thermal carpet cloaks with natural bulk material, International Journal of Heat and Mass Transfer 141 (2019) 487–490.

[14] R. Hu, S. Zhou, Y. Li, D.-Y. Lei, X. Luo, C.-W. Qiu, Illusion thermotics, Advanced Materials 30 (22) (2018) 1707237.

[15] S. Zhou, R. Hu, X. Luo, Thermal illusion with twinborn-like heat signatures, International Journal of Heat and Mass Transfer 127 (2018) 607–613.

[16] S. Huang, J. Zhang, M. Wang, R. Hu, X. Luo, Macroscale thermal diode-like black box with high transient rectification ratio, ES Energy & Environment 6 (2019) 51–6.

[17] L. Xu, J. Huang, Controlling thermal waves with transformation complex thermotics, International Journal of Heat and Mass Transfer 159 (2020) 120133.

[18] S. Narayana, Y. Sato, Heat flux manipulation with engineered thermal materials, Physical Review Letters 108 (21) (2012) 214303.

[19] Q. Ji, X. Chen, J. Liang, V. Laude, S. Guenneau, G. Fang, M. Kadic, Designing thermal energy harvesting devices with natural materials through optimized microstructures, International Journal of Heat and Mass Transfer 169 (2021) 120948.

[20] Q. Ji, G. Fang, J. Liang, Achieving thermal concentration based on fiber reinforced composite microstructures design, Journal of Physics D: Applied Physics 51 (31) (2018) 315304.

[21] T. Han, X. Bai, D. Gao, J. T. Thong, B. Li, C.-W. Qiu, Experimental demonstration of a bilayer thermal cloak, Physical Review Letters 112 (5) (2014) 054302.

[22] H. Xu, X. Shi, F. Gao, H. Sun, B. Zhang, Ultrathin three-dimensional thermal cloak, Physical Review Letters 112 (5) (2014) 054301.

[23] G. Xu, X. Zhou, J. Zhang, Bilayer thermal harvesters for concentrating temperature distribution, International Journal of Heat and Mass Transfer 142 (2019) 118434.

[24] X. Zhou, G. Xu, H. Zhang, Binary masses manipulation

with composite bilayer metamaterial, Composite Structures 267 (2021) 113866.
[25] X. Zhang, X. He, L. Wu, Ellipsoidal bifunctional thermal-electric transparent device, Composite Structures 234 (2020) 111717.
[26] X. He, L. Wu, Thermal transparency with the concept of neutral inclusion, Physical Review E 88 (3) (2013) 033201.
[27] X. Zhang, X. He, L. Wu, A bilayer thermal-electric camouflage device suitable for a wide range of natural materials, Composite Structures 261 (2021) 113319.
[28] Q. Ji, X. Chen, G. Fang, J. Liang, X. Yan, V. Laude, M. Kadic, Thermal cloaking of complex objects with the neutral inclusion and the coordinate transformation methods, AIP Advances 9 (4) (2019) 045029.
[29] G. V. Alekseev, D. A. Tereshko, Particle swarm optimization-based algorithms for solving inverse problems of designing thermal cloaking and shielding devices, International Journal of Heat and Mass Transfer 135 (2019) 1269–1277.
[30] P. Jin, S. Yang, L. Xu, G. Dai, J. Huang, X. Ouyang, Particle swarm optimization for realizing bilayer thermal sensors with bulk isotropic materials, International Journal of Heat and Mass Transfer 172 (2021) 121177.
[31] G. Fujii, Y. Akimoto, M. Takahashi, Exploring optimal topology of thermal cloaks by cma-es, Applied Physics Letters 112 (6) (2018) 061108.
[32] G. Fujii, Y. Akimoto, Optimizing the structural topology of bifunctional invisible cloak manipulating heat flux and direct current, Applied Physics Letters 115 (17) (2019) 174101.
[33] G. Fujii, Y. Akimoto, Topology-optimized thermal carpet cloak expressed by an immersed-boundary level-set method via a covariance matrix adaptation evolution strategy, International Journal of Heat and Mass Transfer 137 (2019) 1312–1322.
[34] G. Fujii, Y. Akimoto, Cloaking a concentrator in thermal conduction via topology optimization, International Journal of Heat and Mass Transfer 159 (2020) 120082.
[35] W. W. Ahmed, M. Farhat, X. Zhang, Y. Wu, Deterministic and probabilistic deep learning models for inverse design of broadband acoustic cloak, Physical Review Research 3 (1) (2021) 013142.
[36] B. Liu, L. Xu, J. Huang, Thermal transparency with periodic particle distribution: A machine learning approach, Journal of Applied Physics 129 (6) (2021) 065101.